

# Response to “Comment on Real-Time Observation on Dynamic Growth/Dissolution of Conductive Filaments in Oxide-Electrolyte-Based ReRAM”

Qi Liu, Sun Jun, Hangbing Lv, Shibing Long, Ling Li, Kuibo Yin, Neng Wan, Yingtao Li, Litao Sun, and Ming Liu\*

In our recently published paper,<sup>[1]</sup> we achieved direct visualization of the dynamic growth and dissolution of conductive filaments (CFs) in Ag (or Cu)/ZrO<sub>2</sub>/Pt systems based on in situ transmission electron microscope (TEM) observations. Furthermore, continuous TEM images clearly showed that the CFs start to grow at the Cu/ZrO<sub>2</sub> (or Ag/ZrO<sub>2</sub>) interface and begin to dissolve at the ZrO<sub>2</sub>/Pt interface, which is in contrast to the prediction from the electrochemical metallization (ECM) theory developed for the solid-electrolyte-based ReRAM (also referred to as the ECM cell).<sup>[2,3]</sup> The same direction of CF growth/dissolution had been demonstrated in other ECM cells, including Ag/ $\alpha$ -Si/Pt,<sup>[4]</sup> Cu/ZnO/Pt,<sup>[5]</sup> and Cu/P3HT:PCBM/ITO devices.<sup>[6]</sup> In our paper,<sup>[1]</sup> we suggested that the differences in cation solubility and diffusion coefficient between traditional solid-electrolyte and oxide-electrolyte materials accounts for this discrepancy, and based on our suggestion, the metal ions would be reduced and crystallized inside the ZrO<sub>2</sub>-electrolyte system in order to explain the observed results.

Valov and Waser made a comment to dispute our explanation based on the following arguments. (1) The EDX analysis presented in our paper cannot identify the chemical valence of Ag (Cu) species inside the CF region. They suggested that the resistive switching (RS) behavior in our device cannot rule out valence change memory (VCM) effects due to oxide materials like ZrO<sub>2</sub>, TiO<sub>2</sub>, HfO<sub>2</sub>, and Ta<sub>2</sub>O<sub>5</sub> which are often used for ECM and VCM cells. (2) The large amount of electrons in the solid materials is not a sufficient condition to reduce the incoming metal ions inside the solid electrolyte materials. (3) Considering the electric potential distribution, the Cu or Ag CFs should not start to grow at the Cu/ZrO<sub>2</sub> (or Ag/ZrO<sub>2</sub>) interface and begin to dissolve at the ZrO<sub>2</sub>/Pt interface. At the end of their comment, they presented a hypothesis in which the growth and dissolution of CF in ZrO<sub>2</sub> result from the metal ion doping/

dedoping effect, and the CF is constituted of the electronically conductive ternary phase with Ag<sup>+</sup> (Cu<sup>2+</sup>) doped ZrO<sub>2</sub>. After carefully analyzing our experimental results, we believe that the explanation presented in our paper is reasonable. The point-by-point response to the comments of Valov and Waser is presented as follows.

- (1) The chemical composition of the CFs is the crucial issue for identifying whether our Cu (Ag)/ZrO<sub>2</sub>/Pt devices belong to the ECM cells. Based on EDX analysis (Figure 2e and Figure 3I in our published paper),<sup>[1]</sup> we recognized that the change of Ag (Cu) signal intensity in different resistive states only can prove that the CF region contains a number of Ag (Cu) species, and cannot directly identify the valence of the Ag (Cu) element inside the CF region. However, we still believe that the CFs observed in our experiment are mainly composed of Ag (Cu) metallic phase on the basis of the previous studies.<sup>[4,7–14]</sup> Many reports have shown that the physical nature of the CF in the ECM cells, which consists of either traditional-solid-electrolyte materials or oxide-solid-electrolyte materials, is Ag (Cu) metallic nanowire, clusters or nanocrystal chains, through studying the lattice structure<sup>[7–9,15,16]</sup> or resistance-temperature characteristics of the CF.<sup>[10–14]</sup> To characterize the physical nature of the CF, the ON-state resistance ( $R_{ON}$ ) of the Cu/ZrO<sub>2</sub>/Pt and Ag/ZrO<sub>2</sub>/Pt devices is measured as a function of temperature. For simplicity, we discuss the Cu/ZrO<sub>2</sub>/Pt device as an example because both devices showed similar resistance-temperature characteristics. As shown in Figure 1,  $R_{ON}$  increases linearly

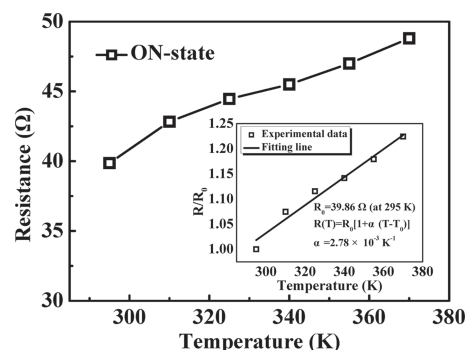


**Figure 1.** Temperature dependence of the ON-state resistance of the Cu/ZrO<sub>2</sub>/Pt device. The inset shows that the resistance temperature coefficient ( $\alpha$ ) of the ON-state device is  $2.78 \times 10^{-3} \text{ K}^{-1}$  at a reference temperature  $T_0 = 295 \text{ K}$ . The value of  $\alpha$  is consistent with that of the Cu nanowire with diameter  $\geq 15 \text{ nm}$ .

Dr. Q. Liu, Dr. H. Lv, Prof. S. Long, Prof. L. Li,  
Dr. Y. Li, Prof. M. Liu  
Lab of Nanofabrication and Novel Device Integration  
Institute of Microelectronics  
Chinese Academy of Sciences  
Beijing 100029, China  
E-mail: liuming@ime.ac.cn  
S. Jun, Dr. K. Yin, Dr. N. Wan, Prof. L. Sun  
SEU-FEI Nano-Pico Center  
Key Laboratory of MEMS of Ministry of Education  
Southeast University  
Nanjing 210096, China



DOI: 10.1002/adma.201203771

with temperature from 295 to 370 K, which is typical electronic transport behavior in metals, indicating that the CF in the Cu/ZrO<sub>2</sub>/Pt device is in a metallic phase. At the same time, we can calculate the resistance temperature coefficient ( $\alpha$ ) of the CF in the Cu/ZrO<sub>2</sub>/Pt device could be calculated as  $\alpha = 2.78 \times 10^{-3} \text{ K}^{-1}$  at  $T_0 = 295 \text{ K}$ , on the basis of the resistance-temperature dependence ( $R(T) = R_0[1 + \alpha(T - T_0)]$ , where  $R_0$  is the resistance at temperature  $T_0$  and  $\alpha$  is the resistance temperature coefficient.<sup>[11]</sup> It is worth noting that the  $\alpha$  of CF in different Cu-based ECM cells (for example, the  $\alpha$  of CF is from  $2.39 \times 10^{-3}$  to  $2.98 \times 10^{-3} \text{ K}^{-1}$  in Cu/ZrO<sub>2</sub>:Cu/Pt,<sup>[11]</sup>  $2.26 \times 10^{-3} \text{ K}^{-1}$  in Cu/ZnO/Pt<sup>[13]</sup> and  $2.02 \times 10^{-3} \text{ K}^{-1}$  in Cu/HfO<sub>2</sub>:Cu/Pt,<sup>[14]</sup> respectively) is almost equal to that of the Cu nanowire with diameter  $\geq 15 \text{ nm}$  ( $\alpha = 2.5 \times 10^{-3} \text{ K}^{-1}$ ),<sup>[17]</sup> indicating that the CF is composed of Cu in a metallic state. It should also be pointed out that the possibility that the Ag<sup>+</sup> (Cu<sup>+</sup> or Cu<sup>2+</sup>) might exist in the CF region cannot be ruled out by the EDX results and the relationship between  $R_{ON}$  and temperature. However, these results can confirm that Ag (Cu) metallic phase exists in the CF region and the current in the ON-state device is mainly transported through the Ag (Cu) metallic phase paths. Hence, we believe that our interpretation for the TEM observations based on the formation and dissolution of Ag (Cu) CFs is reasonable.

It is suggested here that it is impossible that electron irradiation effects impact on the reliability of our in situ TEM experiment results. In our previous studies on Ag/ZnO:Mn/Pt and Ag/ZrO<sub>2</sub>/Cu NC/Pt devices, Ag CF has been observed to possess a similar conical shape (the cone top was connected to the Pt electrode in ex situ TEM specimens).<sup>[12,18]</sup> The specimens were fabricated after the devices were switched to the ON-state. Similar results in the ex situ and in situ TEM experiments confirm that the CF conical morphology is a natural property of the RS materials and the impact of electron irradiation effects can be excluded. In the elemental mapping (Figure S1 in the Supporting Information of our paper),<sup>[1]</sup> the Zr signal intensity is not obviously attenuated in the CF region due to the low testing time. The total testing time was about 40 min to obtain the image shown in Figure S1 and the time for which the electron beam spot stayed at each pixel point was only about 0.5 s. In this case, the change of the Zr signal intensity is difficult to observe because there is still a lot of ZrO<sub>2</sub> material wrapped around the CF.

(2) We agree with Valov and Waser that the incoming electron needs to overcome a potential barrier to reduce the M<sup>Z+</sup> cations in the ZrO<sub>2</sub> layer. The average energy of the injecting electron from the cathode is dependent on the external applied voltage. When the applied voltage is increased, some electrons with high energy can overcome the reduced potential barrier to react with the M<sup>Z+</sup>, resulting in the M<sup>Z+</sup> cations reducing back to M atoms ( $M^{Z+} + Ze^- \rightarrow M$ ). Using first-principle calculations, the formation energy of substitutional Ag (Cu) is far higher than that of interstitial Ag (Cu) in the ZrO<sub>2</sub> lattice (shown in Table 1), indicating that the Ag (Cu) ions prefer to exist in the interstitial position of the ZrO<sub>2</sub> lattice. The compensation for the additional incorporation of interstitial Ag<sup>+</sup> (Cu<sup>2+</sup>) ions can be proceeded by electrons rather than additional oxygen vacancies. Under the closed circuit conditions, the Ag<sup>+</sup> (Cu<sup>2+</sup>) ions incorporated into the

**Table 1.** The formation energy of the Ag (Cu) doped ZrO<sub>2</sub> systems. R indicates that one doping metal atom replaces one Zr atom. lx, ly and lz indicate that one doping metal atom exists in the different interstitial sites.

Sites	Formation Energy [eV]	
	Ag doped ZrO <sub>2</sub>	Cu doped ZrO <sub>2</sub>
R	12.0079	10.9614
lx	5.0138	3.4924
ly	5.0029	3.5158
lz	5.0132	3.4913

ZrO<sub>2</sub> layer are immediately matched by the electrons from the cathode with the same amount of charge, which will keep the overall electroneutrality of the system. Based on the above analyses, we suggested that the Ag (Cu) ion reduction reaction can occur inside the ZrO<sub>2</sub> material.

(3) The oxidation and reduction reaction is dominated by the electrochemical potential, which is described as  $\mu = \mu^0 + F\Phi + RT \ln(\gamma C)$  (where  $\mu^0$  is the chemical potential at  $\gamma C = 1$ ;  $F$ ,  $\Phi$ ,  $R$ ,  $T$ ,  $\gamma$ , and  $C$  are the Faraday constant, electrical potential, molar gas constant, temperature, activity coefficient, and concentration of the metal cation, respectively).<sup>[19]</sup> From this equation, it can be deduced that the redox reaction is influenced by not only the applied voltage but also the cation concentration. Taking Cu as an example, the activation energies of reduction ( $E_R$ : Cu<sup>Z+</sup>  $\rightarrow$  Cu,  $z = 1$  or 2) and oxidation ( $E_O$ : Cu  $\rightarrow$  Cu<sup>Z+</sup>) at the Cu/ZrO<sub>2</sub> interface are equal at equilibrium without any bias application. When a positive bias is applied to the Cu electrode, the Cu<sup>Z+</sup> cations produced in the Cu electrode will drift toward the Cu/ZrO<sub>2</sub> interface along with the electrical field, leading to  $E_R$  becoming smaller than  $E_O$  due to the increase in the Cu<sup>Z+</sup> concentration. Simultaneously, a large number of incoming electrons will reach the anode from the cathode through the ZrO<sub>2</sub> film due to the fast migration velocity. As a result, the reduction rate (Cu<sup>Z+</sup>  $\rightarrow$  Cu) will be larger than the oxidation rate (Cu  $\rightarrow$  Cu<sup>Z+</sup>) at the Cu/ZrO<sub>2</sub> interface. With the continuation of the process, the successive accumulation of Cu atoms at the Cu/ZrO<sub>2</sub> interface leads to the nucleation of the Cu CF at some local region of the anode/ZrO<sub>2</sub> interface, and then grows toward the Pt cathode. On the other hand, applying a negative bias voltage to the Cu electrode induces the migration of Cu<sup>Z+</sup> cations generated in the CF region in the ZrO<sub>2</sub> layer towards the bottom of the Cu electrode, leading to a decrease in Cu<sup>Z+</sup> concentration at the ZrO<sub>2</sub>/Pt interface. Consequently,  $E_O$  becomes smaller than  $E_R$ , promoting the oxidation and shrinkage of the Cu filament. The kinetics of the CF formation and dissolution in our device are similar to the gap-type atomic switches.<sup>[19]</sup>

(4) We are afraid that the explanation offered by Valov and Waser in their comment is inconsistent with our experimental results. Firstly, in contrast to the Ca<sup>2+</sup> and Y<sup>3+</sup> ion doping in the ZrO<sub>2</sub>, the Cu<sup>2+</sup> and Ag<sup>+</sup> ions are difficult to replace the Zr<sup>4+</sup> ion sites in the ZrO<sub>2</sub> sublattice due to their higher Gibbs free energy ( $\Delta G_0$ ). The  $\Delta G_0$  values are  $-1039.724 \text{ kJ/mol}$ ,  $-128.292 \text{ kJ/mol}$ ,  $-147.886 \text{ kJ/mol}$ , and  $-11.184 \text{ kJ/mol}$  for ZrO<sub>2</sub>, CuO, Cu<sub>2</sub>O, and Ag<sub>2</sub>O, respectively.<sup>[20]</sup> The first-principle

calculation results confirmed that the  $\text{Ag}^+$  ( $\text{Cu}^{2+}$ ) ions prefer to exist in the interstitial positions of the  $\text{ZrO}_2$  lattice. Hence, the incorporation of  $\text{Ag}^+$  ( $\text{Cu}^{2+}$ ) ions in the  $\text{ZrO}_2$  cannot introduce additional oxygen vacancies. Secondly, the resistance-temperature dependence demonstrated that the CF in our device is in the metallic phase. If the CF is composed of the electronically conductive ternary phase with  $\text{Ag}^+$  ( $\text{Cu}^{2+}$ ) doped  $\text{ZrO}_2$ , the electrons should transport through the CF by hopping from  $\text{Ag}^+$  ( $\text{Cu}^{2+}$ ) ions. In this case, the relationship between  $R_{\text{ON}}$  and temperature is not metallic.

In conclusion, the comments by Valov and Waser offer a valuable opportunity to further elucidate the mechanism of the CF growth/dissolution in  $\text{ZrO}_2$ -based ECM cells. Based on the temperature coefficient results, we are convinced that the CF observed in our experiment mainly consists of a Ag (Cu) metal phase chain. Through an in-depth discussion, we reaffirm that the direction of the CF growth/dissolution is dominated by the redox reaction of the Ag (Cu) cations inside the  $\text{ZrO}_2$ . However, the resistive switching phenomenon is very complex, which may be caused by the influence of multiple effects. To fully understand the switching mechanism of RRAM, more detailed studies need to be carried out in the future.

## Acknowledgements

Q.L. and S.J. contributed equally to this work. The authors thank Z. H. Chen from the Institute of Semiconductor, Chinese Academy of Sciences for help with the first-principle calculations. This work was supported by the Ministry of Science and Technology of China under grant no. 2011CBA00602, 2010CB934200, 2011CB921804, 2009CB925003, 2011CB707600, 2009CB623702, 2011AA010401, and 2011AA010402 and NSFC under grant no. 60825403, 61106119, 61221004, 61274091, 61106082, 50972160, 51071044, 60976003, and 61006011.

Received: September 10, 2012  
Published online:

- [1] Q. Liu, J. Sun, H. Lv, S. Long, K. Yin, N. Wan, Y. Li, L. Sun, M. Liu, *Adv. Mater.* **2012**, *24*, 1844.
- [2] R. Waser, R. Dittmann, G. Staikov, K. Szot, *Adv. Mater.* **2009**, *21*, 2632.
- [3] I. Valov, R. Waser, J. R. Jameson, M. N. Kozicki, *Nanotechnology* **2011**, *22*, 254003.
- [4] Y. C. Yang, P. Gao, S. Gaba, T. Chang, X. Pan, W. Lu, *Nat. Commun.* **2012**, *3*, 732.
- [5] S. Peng, F. Zhuge, X. Chen, X. Zhu, B. Hu, L. Pan, B. Chen, R.-W. Li, *Appl. Phys. Lett.* **2012**, *100*, 072101.
- [6] S. Gao, C. Song, C. Chen, F. Zeng, F. Pan, *J. Phys. Chem. C* **2012**, *116*, 17955.
- [7] C.-P. Hsiung, H.-W. Liao, J.-Y. Gan, T.-B. Wu, J.-C. Hwang, F. Chen, M. J. Tsai, *ACS Nano* **2010**, *4*, 5414.
- [8] Z. Xu, Y. Bando, W. Wang, X. Bai, D. Golberg, *ACS Nano* **2010**, *4*, 2515.
- [9] T. Fujii, M. Arita, Y. Takahashi, I. Fujiwara, *Appl. Phys. Lett.* **2011**, *98*, 212104.
- [10] T. Sakamoto, K. Lister, N. Banno, T. Hasegawa, K. Terabe, M. Aono, *Appl. Phys. Lett.* **2007**, *91*, 092110.
- [11] W. Guan, M. Liu, S. Long, Q. Liu, W. Wang, *Appl. Phys. Lett.* **2008**, *93*, 223506.
- [12] Y. C. Yang, F. Pan, Q. Liu, M. Liu, F. Zeng, *Nano Lett.* **2009**, *9*, 1636.
- [13] F. Zhuge, S. Peng, C. He, X. Zhu, X. Chen, Y. Liu, R.-W. Li, *Nanotechnology* **2011**, *22*, 275204.
- [14] Y. Wang, Q. Liu, S. Long, W. Wang, Q. Wang, M. Zhang, S. Zhang, Y. Li, Q. Zuo, J. Yang, M. Liu, *Nanotechnology* **2010**, *21*, 045202.
- [15] S. Z. Rahaman, S. Maikap, W. S. Chen, H. Y. Lee, F. T. Chen, T. C. Tien, M. J. Tsai, *J. Appl. Phys.* **2012**, *111*, 063710.
- [16] S. Z. Rahaman, S. Maikap, W. S. Chen, H. Y. Lee, F. T. Chen, M. J. Kao, M. J. Tsai, *Appl. Phys. Lett.* **2012**, *101*, 073106.
- [17] Aveek Bid, Achyut Bora, A. K. Raychaudhuri, *Phys. Rev. B* **2006**, *74*, 035426.
- [18] Q. Liu, S. Long, H. Lv, W. Wang, J. Niu, Z. Huo, J. Chen, M. Liu, *ACS Nano* **2010**, *10*, 6162.
- [19] T. Hino, T. Hasegawa, K. Terabe, T. Tsuruoka, A. Nayak, T. Ohno, M. Aono, *Sci. Technol. Adv. Mater.* **2011**, *12*, 013003.
- [20] I. Barin, *Thermochemical Data of Pure Substances*, Wiley-VCH, Weinheim, Germany **1995**.